ORIGINAL PAPER

RJME
Romanian Journal of Morphology & Embryology
http://www.rjme.ro/

Iron oxide nanoparticles modulate the interaction of different antibiotics with cellular membranes

CLAUDIA MIHAELA ISTRATE[1)], ALINA MARIA HOLBAN[2,3)], ALEXANDRU MIHAI GRUMEZESCU[2)], LAURENŢIU MOGOANTĂ[4)], GEORGE DAN MOGOŞANU[5)], TUDOR SAVOPOL[1)], MIHAELA MOISESCU[1)], MINODORA IORDACHE[1)], BOGDAN ŞTEFAN VASILE[2)], EUGENIA KOVACS[1)]

[1)]*Department of Biophysics and Cellular Biotechnology, "Carol Davila" University of Medicine and Pharmacy, Bucharest, Romania*

[2)]*Department of Science and Engineering of Oxide Materials and Nanomaterials, Faculty of Applied Chemistry and Materials Science, Politehnica University of Bucharest, Romania*

[3)]*Department of Microbiology–Immunology, Faculty of Biology, University of Bucharest, Romania*

[4)]*Research Center for Microscopic Morphology and Immunology, University of Medicine and Pharmacy of Craiova, Romania*

[5)]*Department of Pharmacognosy & Phytotherapy, Faculty of Pharmacy, University of Medicine and Pharmacy of Craiova, Romania*

Abstract

The interaction of nanomaterials with cells and lipid bilayers is critical in many applications such as phototherapy, imaging and drug/gene delivery. These applications require a firm control over nanoparticle–cell interactions, which are mainly dictated by surface properties of the nanoparticles. The aim of this study was to investigate the interaction of Fe_3O_4 nanoparticles functionalized with several wide use antibiotics with opossum kidney (OK) cellular membranes in order to reveal changes in the membrane organization at different temperatures. We also investigated the *in vivo* biodistribution of the tested nanoparticles in a mouse model. Our results showed that, at low temperatures (31–35^{0}C), plain Fe_3O_4 nanoparticles induced a drop of the membrane fluidity, while at physiological or higher temperatures (37–39^{0}C) the membrane fluidity was increased. On the other hand, when nanoparticles functionalized with the tested antibiotics were used, we observed that the effect was opposite as compared to control Fe_3O_4 nanoparticles. Although most of antibiotics, used as plain solutions or linked on magnetite nanoparticles, proved heterogeneous effect on *in vitro* OK cells membrane fluidity, the aminoglycosides streptomycin and neomycin, used both as plain solutions and also combined with nanoparticles kept the same effect in all experimental conditions, increasing the membrane fluidity of OK cells plasma membrane. *In vivo* results showed that the antibiotic functionalized nanoparticles have a similar biodistribution pattern within the mouse body, being transported through the blood flow and entering the macrophages through endocytosis. Functionalized magnetite nanoparticles manifested a preferential biodistribution pattern, clustering within the lungs and spleen of treated mice. These results demonstrate that antibiotics manifest a different effect on plasma membrane fluidity depending on their type and temperature. Magnetite nanoparticles may interfere with antibiotic-cellular interactions by changing the plasma membrane fluidity. The fact that the antibiotic functionalized magnetite nanoparticles have a similar biodistribution pattern, are transported through the blood flow, and they increase the cellular uptake of the drug, suggest that they may be used for further studies aiming to develop personalized targeted delivery and controlled release nanoshuttles for treating localized and systemic infections.

Keywords: magnetite nanoparticles, drug delivery, OK cells, biodistribution, iron oxide, cell membrane.

Introduction

The first step in the biochemical pathway of any drug action is its interaction with the cellular membrane. If this interaction is weak, this can constitute a rate-limiting step, drastically lowering the efficiency of the drug [1]. The plasma membrane is a semi-permeable barrier, which both allows the selective traffic of different molecules and insures the homeostasis of the cellular content [2]. Small and non-polar molecules such as O_2 and CO_2 can readily diffuse across the lipid bilayer; however, polar molecules such as ions and larger nanomaterials are incapable of crossing the plasma membrane on their own and they are usually transported across the lipid bilayer through specialized membrane-transport systems [3].

Many biomedical applications rely on the use of nanostructured materials, especially those with magnetic properties [4, 5]. Surface and core properties of nanoparticles (NPs) can be engineered for their use in imaging [6], drug/gene delivery [7], biosensing [8], diagnosis of many diseases [9] and various other applications [10, 11]. The delivery of many NPs faces challenges associated with toxicity of surface ligands, the range of cell lines they are exposed to and serum conditions. Cationic NPs interact with cell membranes strongly as compared to anionic and zwitterionic ones [12], but are very toxic and immunogenic. These NPs are also prone to interact with serum proteins present in blood, thereby altering delivery profiles of NPs [13]. Therefore, the choice of surface coating of NPs is important to lower toxicity and immunogenicity while increasing transport and delivery efficiency [14].

Iron oxide NPs are largely used in magnetic resonance imaging (MRI) [14], magnetic field induced thermal therapy [15], various systems like NP-loaded liposomes [16], magnetite-doped microspheres and magnetic fluids (ferrofluids) [17, 18].

The nanoparticles enter the cell by endocytosis and

the neutral and negatively charged nanoparticles are much less adsorbed on the negatively charged cell-membrane surface and consequently show lower levels of internalization as compared to the positively charged particles [19–21].

Villanueva *et al.* [22] have studied the uptake of iron oxide nanoparticles (with similar aggregate sizes) functionalized with charged differently carbohydrates in human cervical carcinoma cell lines (HeLa). They did not observe any cellular uptake of neutral nanoparticles, however, the negatively charged nanoparticles showed uptake and toxicity depending on the type of surface coating. Non-ionic iron oxide nanoparticles without surface coatings have also shown a high level of internalization by interacting strongly and non-specifically with the plasma membrane as observed through complementary magnetic assays, magnetophoresis (MP), and electron-spin resonance (ESR) [23]. The internalization of negatively charged nanoparticles is believed to occur through non-specific binding and clustering of the particles on cationic sites on the plasma membrane, followed by endocytosis [20].

Although there can be found several studies reporting the ability of magnetite nanoparticles to behave as efficient shuttles to enhance the efficiency of antibiotics, there are no reports regarding the close interaction between antibiotic functionalized magnetite and cellular plasma membranes.

In this study, we used five aminoglycosides (kanamycin, gentamicin, amikacin, streptomycin and neomycin), three *β*-lactam (penicillin, amoxicillin, cefotaxime), a macrolide (erythromycin), two polymyxins (bacitracin, polymyxin) and one glycopeptide (vancomycin) to functionalize magnetite nanoparticles and to analyze the effect of these nanoformulations on the membrane fluidity at different temperatures. We used 1-(4-trimethylammoniumphenyl)-6-phenyl-1,3,5-hexatriene *p*-toluenesulfonate (TMA-DPH) for recording the fluorescence anisotropy of membranes in cell suspensions treated either with antibiotics alone or fused with magnetite nanoparticles at different temperatures, in order to observe if hypothermia or fever play a role in the drugs uptake. We choose to use nanoparticles fused with antibiotics because they carry a small amount of antibiotic and keep the active drug efficiency, which makes them less toxic than simple antibiotics. This is a very important feature in the case of patients that are supposed to be treated with antibiotics for long periods. We also tested the biocompatibility and biodistribution of the obtained antibiotics/magnetite nanostructures using an *in vivo* mouse model.

Materials and Methods

Materials

Ferrous sulfate 7-hydrate ($FeSO_4 \cdot 7H_2O$), ferric chloride ($FeCl_3$), ammonia (NH_3, 25%), gentamicin (GEM), kanamycin (KAN), amikacin (AMI), penicillin (PEN), polymyxin (POL), neomycin (NEO), cefotaxime (CEF), bacitracin (BAC), amoxicilin (AMO), erythromycin (ERI), streptomycin (STR), vancomycin (VAN), dimethyl sulfoxide (DMSO) were purchased from Sigma-Aldrich. All chemicals were of analytical purity and used with no further purification.

Preparation of antibiotics functionalized magnetite nanoparticles

Magnetite nanoparticles functionalized with different therapeutic agents (GEM, KAN, AMI, PEN, POL, NEO, CEF, BAC, AMO, ERI, STR, VAN) were prepared and characterized by TEM, XRD and TGA according to our previously published papers [4, 24–26]. Briefly, a solution consisting of antibiotic and NH_4OH were prepared in 200 mL deionized water and added drop by drop into 400 mL aqueous solution of Fe^{2+}/Fe^{3+} under vigorous string. pH of the solution was maintained at 9. A black precipitate was obtained and separated by a strong NdFeB permanent magnet and repeatedly washed with deionized water. One mg of each prepared nanopowder was dispersed in 1 mL of deionized water for further biological assays.

Characterization of antibiotics functionalized magnetite nanoparticles

The transmission electron microscopy (TEM) images were obtained on finely powdered samples using a Tecnai™ G2 F30 S-TWIN high-resolution transmission electron microscope from FEI Company (OR, USA) equipped with Selected Area Electron Diffraction (SAED). The microscope was operated in transmission mode at 300 kV with TEM point resolution of 2 Å and line resolution of 1 Å. The prepared powders were dispersed into pure ethanol and ultrasonicated for 15 minutes. After that, the diluted sample was put onto a holey carbon-coated copper grid and left to dry before TEM analysis.

X-ray diffraction analysis was performed on a Shimadzu XRD 6000 diffractometer at room temperature. In all the cases, Cu Kα radiation from a Cu X-ray tube (run at 15 mA and 30 kV) was used. The samples were scanned in the Bragg angle *2h* range of 10–80.

The thermogravimetric (TG) analysis of the prepared samples was assessed with a Shimadzu DTG-TA-50H instrument. Samples were screened to 200 mesh prior to analysis, were placed in alumina crucible, and heated with 10 K/min. from room temperature to 800^0C, under the flow of 20 mL/min. dried synthetic air (80% N_2 and 20% O_2).

Cell cultures

For the membrane fluidity tests, we used opossum kidney (OK) cells because they have pharmacological sensitivity to aminoglycoside antibiotics, similar to inner ear sensory cells. OK cells were purchased from the American Type Culture Collection (Manassas, VA). The cells were cultured in antibiotic-free Dulbecco's Modified Eagle's Medium with 2 mM L-glutamine and 4.5 g/L glucose (PAA, Austria) supplemented with 10% fetal bovine serum (Gibco, Scotland, UK), at 37^0C, 5% CO_2. Subconfluent cells were harvested by trypsination (0.05% *w/v* Trypsin–4Na^+EDTA, Biochrom AG, Germany).

Fluorescence anisotropy measurements performed on OK cells

The fluorescence anisotropy of lipophilic probes dissolved in a membrane is directly related to micro-fluidity of lipid environment. Fluorescence anisotropy (*r*) is defined as:

$$r = \frac{I_{VV} - GI_{VH}}{I_{VV} + 2GI_{VH}}$$

where the fluorescence intensities (I) are recorded in polarized light at λ_{ex}=385 nm and λ_{em}=427 nm, with polarizers oriented as specified by the indices (V – vertical, H – horizontal); G (defined as I_{HV}/I_{HH}) is a correction factor related to the measuring system. Higher values of the fluorescence anisotropy correspond to a more rigid (or less fluid) environment.

The fluorescence anisotropy may theoretically vary between 0 and 1. However, some considerations related to the statistics thermal movement of the probe, limit the anisotropy to lower values ($r_{max} \leq 0.4$) [27].

Subconfluent OK cultured cells were washed with phosphate buffered saline (PBS), trypsinized and centrifuged at 250×g for 5 minutes; the resulting pellet was re-suspended in PBS at a cell density equivalent to an optical density of 0.18 at 450 nm. Two mL of cell suspension were then incubated with 1 μM TMA-DPH (final concentration) for five minutes and subsequently with 500 μg/mL (final concentration) of antibiotics for five minutes.

I_{VV} and I_{VH} were measured simultaneously for each sample in the 31–39^{0}C temperature range.

In vivo biocompatibility and biodistribution

Three weeks old Balb/c mice were injected aseptically with 200-μL of antibiotics functionalized magnetite and the mice were kept in standard conditions for 72 hours, before the organs removal.

The experimental protocol was applied according with the European Council Directive No. 86/609/24 November 1986, the European Convention on the Protection of Vertebrate Animals (2005) and the Romanian Government Ordinance No. 37/2 February 2002.

The mice organs were collected under general anesthesia. Biological material was fixed, directly after the sampling, in 10% buffered neutral formalin, for 72 hours, at room temperature, and then processed for routinely histological paraffin embedding technique.

For the histological study of nanoparticles, 4-μm thick serial sections were cut on a MICROM HM355s rotary microtome (MICROM International GmbH, Walldorf, Germany) equipped with a waterfall based section transfer system (STS, MICROM).

The cross-sections were placed on histological blades treated with poly-L-Lysine (Sigma-Aldrich, Munich, Germany).

After Hematoxylin–Eosin (HE) classical staining, cross-sections were evaluated and photographed using a Nikon Eclipse 55i light microscope equipped with a Nikon DS–Fi1 CCD high definition video camera (Nikon Instruments, Apidrag, Bucharest, Romania).

Images were captured, stored and analyzed using Image ProPlus 7 AMS software (Media Cybernetics Inc., Marlow, Buckinghamshire, UK) [28].

Statistics

A statistical analysis of experimental data based on two-tailed unpaired Student's t-test was used.

Results

Prepared magnetite nanoparticles functionalized with a series of antimicrobial therapeutic agents were previously characterized by TEM, XRD, TGA. According to TEM analysis, the dimensions of prepared particles do not exceed 10 nm. TEM images of Fe_3O_4@AMI are plotted in Figure 1.

SAED pattern of Fe_3O_4@AMI (Figure 1a) shows a high polycrystalline nature of magnetite without the presence of any other mineral phase. HR-TEM analysis (Figure 1b) confirms the nanometric dimensions of the crystalline powder and reveals on the surface of spherical particles a supplementary phase (shell) with a low degree of crystallinization. Figures 1c and 1d show TEM images of Fe_3O_4@AMI nanoparticles, which were randomly chosen as an example, and they reveal the uniform distribution of diameters without the tendency to form aggregates.

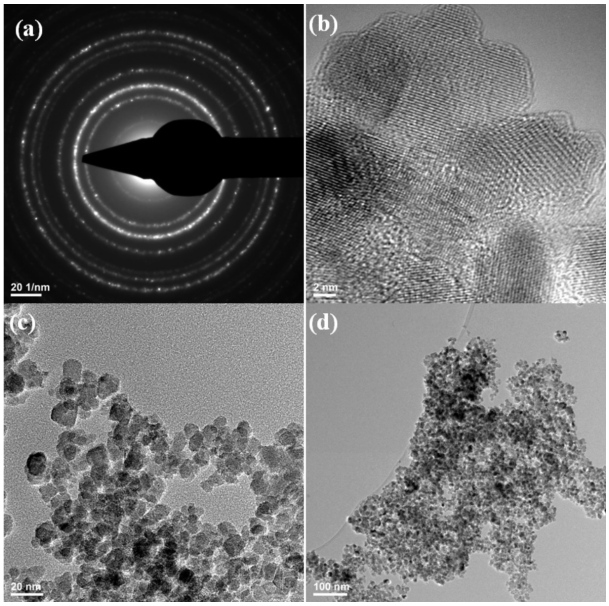

Figure 1 – ***SAED pattern (a), HR-TEM image (b), and TEM images (c and d) of Fe_3O_4@AMI.***

The crystalline nature of magnetite nanoparticles functionalized with antibiotics was confirmed by X-Ray Diffraction (XRD). XRD patterns show a good degree of crystallinity, without any impurities (Figure 2). The identified crystalline phase in all samples was magnetite (JCPDS No. 65–3107) [32].

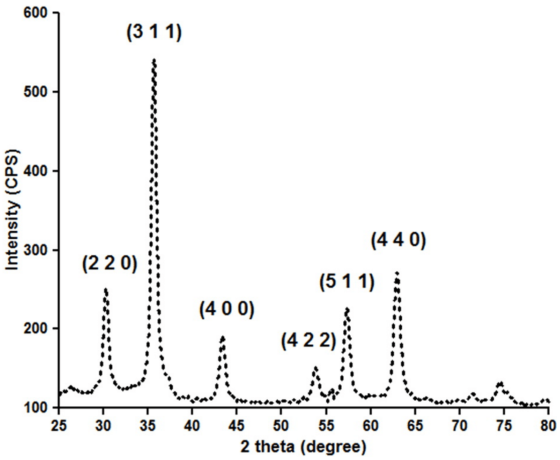

Figure 2 – ***XRD pattern of Fe_3O_4@AMI.***

Thermo-gravimetric analysis was used in order to evaluate the amount of antibiotics that interact with the surface of magnetite nanoparticles. The estimation was performed at 600^{0}C by difference between weight loss of unfunctionalized magnetite nanoparticles and weight loss of antibiotics functionalized magnetite nanoparticles, the amount of therapeutic agent varying from 1 to 6%.

Fluorescence anisotropy measurements demonstrate that OK membrane fluidity is influenced by the used antibiotic, by the presence of nanoparticles and also by the temperature. At temperatures ranging 31–35^{0}C, it was observed a drastic decrease in membrane fluidity for all tested variants (both plain antibiotics solutions and magnetite functionalized with antibiotics). On the other hand, when tests were performed at temperatures between 37–39^{0}C, the results revealed an increase of membrane fluidity (Figures 3 and 4).

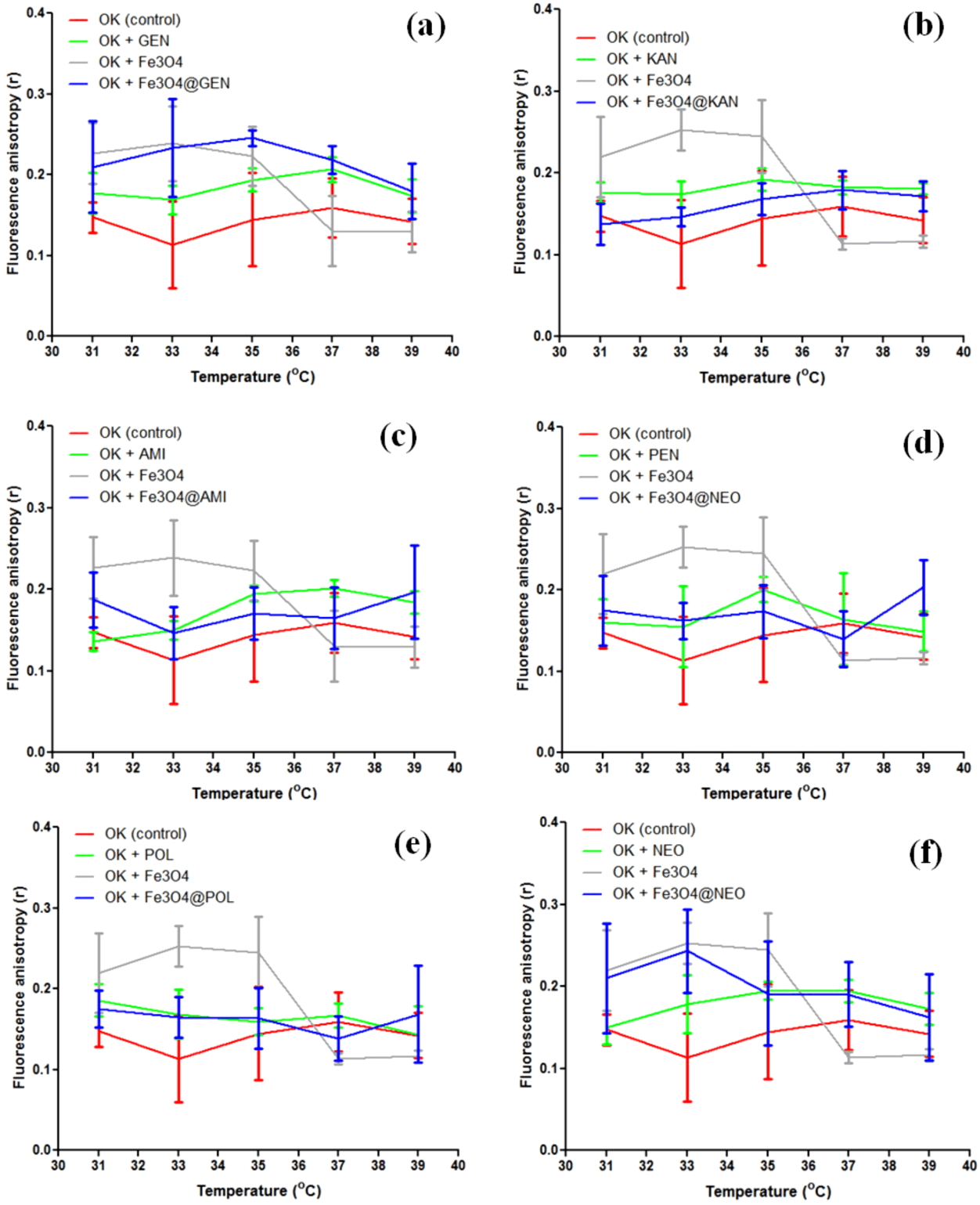

Figure 3 – ***The influence of GEN, Fe_3O_4@GEN, KAN, Fe_3O_4@KAN, AMI, Fe_3O_4@AMI, PEN, Fe_3O_4@PEN, POL, Fe_3O_4@POL, NEO, Fe_3O_4@NEO on OK cells fluorescence anisotropy at different temperatures.***

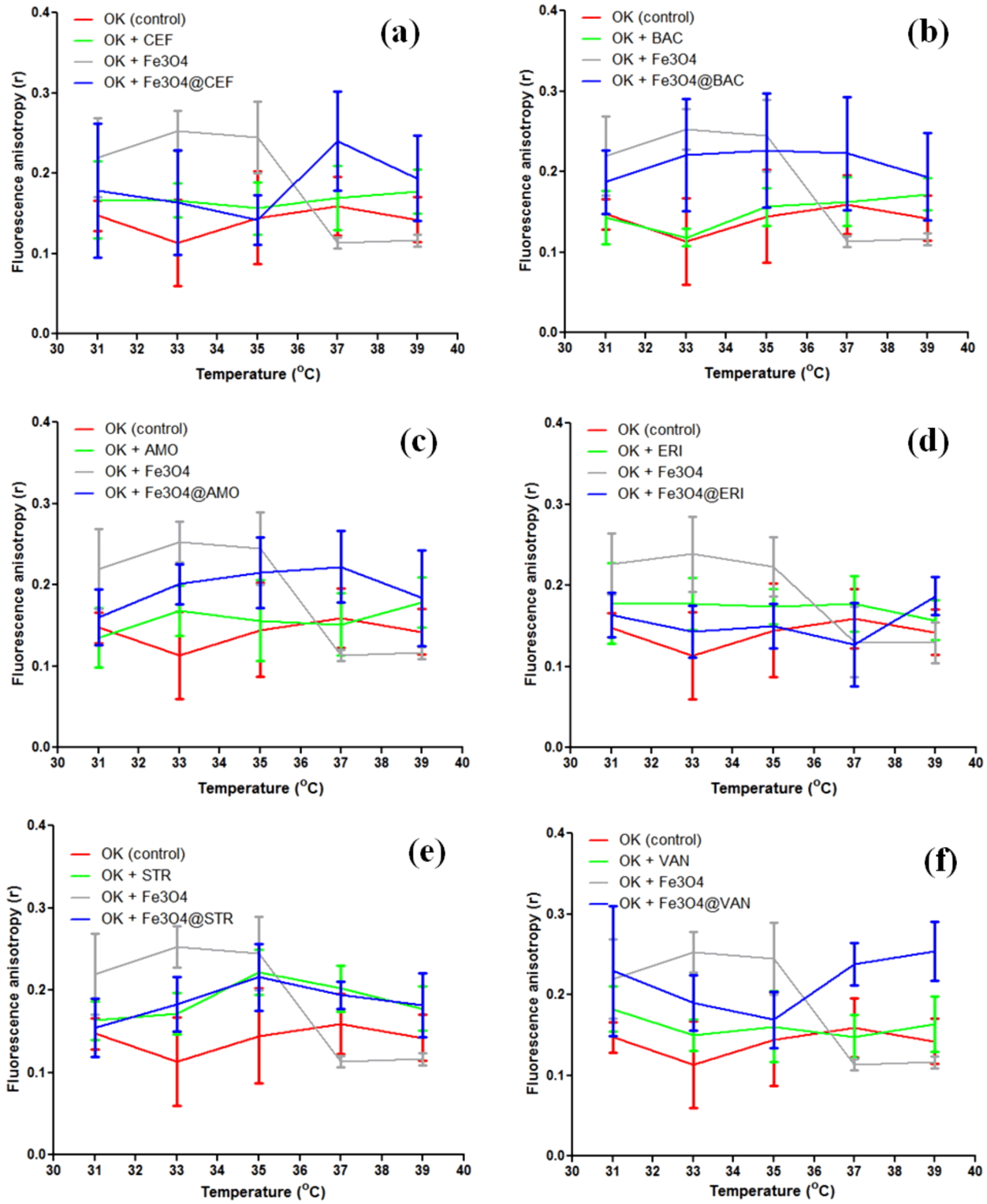

Figure 4 – ***The influence of CEF, Fe_3O_4@CEF, BAC, Fe_3O_4@BAC, AMO, Fe_3O_4@AMO, ERI, Fe_3O_4@ERI, STR, Fe_3O_4@STR, VAN, Fe_3O_4@VAN on OK cells fluorescence anisotropy at different temperatures.***

The most important differences were observed at 37 and 39^{0}C, where nanoparticles functionalized with gentamicin, vancomycin, cefotaxime, bacitracin and amoxicillin induced a decrease in OK cells membrane fluidity as compared with plain antibiotic solutions (Figures 3a, 4a, 4b, 4c and 4f). Amikacin and kanamycin showed a low effect on OK cells membrane fluidity at this temperature range (Figure 3, b and c). Magnetite nanoparticles functionalized with erythromycin as well as polymyxin and penicillin significantly increased OK membrane fluidity at temperatures ranging 37 to 39^{0}C (Figures 3d, 3e and 4d). Of all used antibiotics only the aminoglycosides streptomycin and neomycin both as plain solutions and also combined with nanoparticles proved to keep the same effect in all experimental conditions on the OK cells, increasing their membrane fluidity (Figures 3f and 4e).

In vivo biodistribution results revealed that magnetite nanoparticles functionalized with antibiotics are transported through the blood flow and localize in certain

organs. Intraperitoneally injected nanoparticles from a suspension obtained in sterile PBS were found clustered preferentially within the lungs and spleen (Figure 5, c–e). In the brain, liver and kidney magnetite nanoparticles were absent (Figure 5, a, b, and e).

In the lungs, functionalized magnetite nanoparticles were observed mainly in the perivascular macrophages found in the intra-alveolar septum. Nanoparticles were also found in the intravascular cells belonging to the monocyte-macrophage system. Nanoparticles were present in the spleen sections, but only in the red pulp, being absent in the white pulp (Figure 5f).

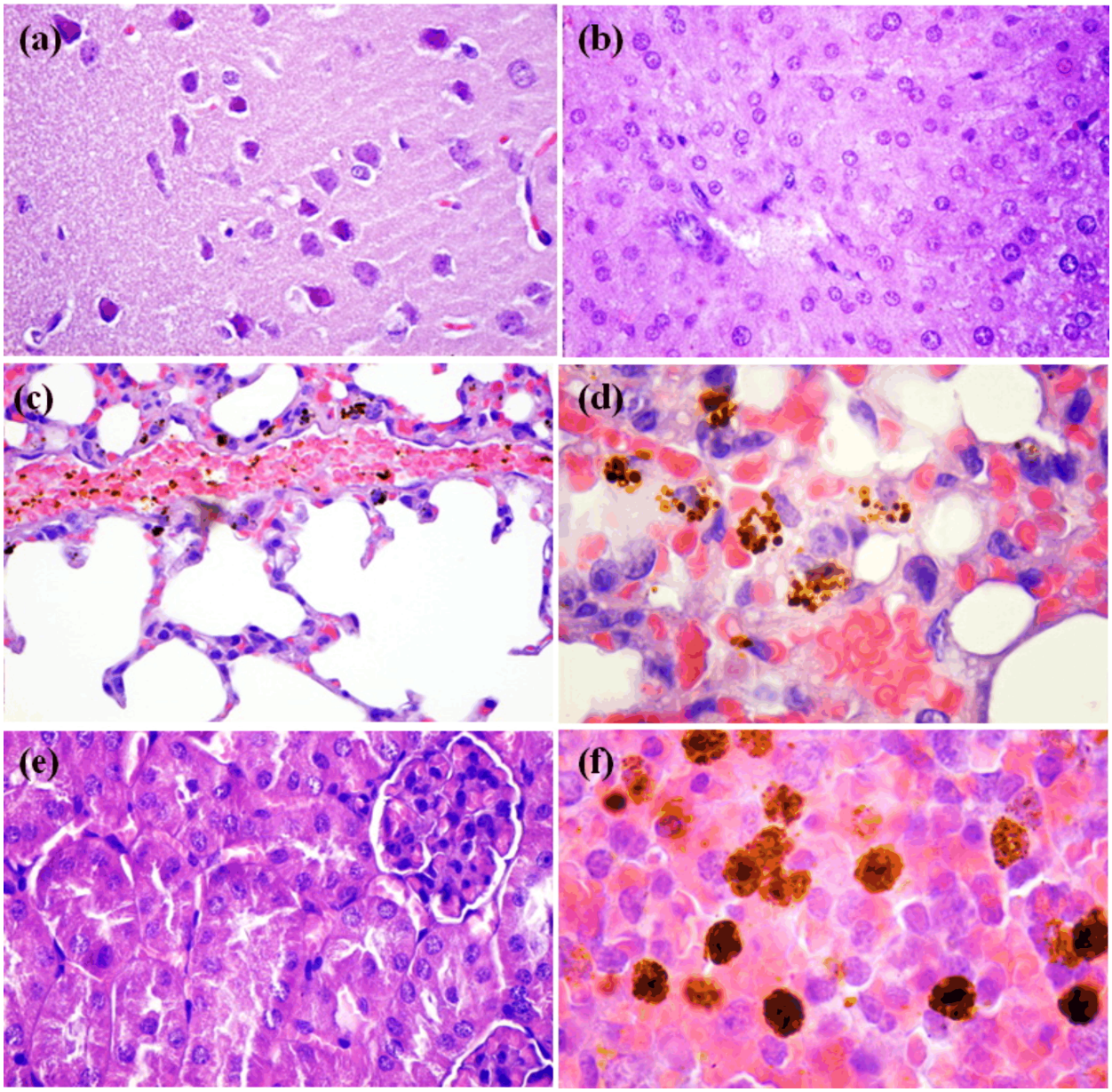

Figure 5 – ***Transversal section through the brain (a), liver (b), lung (c and d), kidney (e), and spleen (f) of a mouse treated with NEO-functionalized magnetite nanoparticles. HE staining: ×400 (a–c, e and f), ×1000 (d).***

Discussion

Biomedical applications of magnetite nanoparticles are in continuous development, starting from anti-tumoral strategies to antimicrobial strategies, due to the versatility of functionalization with different biological molecules [29–32].

The antibiotics used in this study are a large number of aminoglycosides and other antibiotics. We chose antibiotics from different classes to see if there is a difference between them and because they have been used in many studies as functionalizing agents of several nanoparticles that showed a potentiating activity of the antibiotics against some bacterial strains [24–27].

We studied the effect of different types of antibiotics, used both as simple solutions or fused with magnetite nanoparticles on the organization of natural membrane bilayers, using fluorescence anisotropy (r) measurements. The effects of antibiotics alone or fused with nanoparticles on r were monitored at different temperature domains ranging from 31 to 37^0C and from 37 to 39^0C. The choice of these two temperature intervals was based on the observation that the effect of nanoparticles on the membrane fluidity showed an abrupt drop around 37^0C, which is the normal physiological temperature of the studied cells [33]. Below this temperature, the fluidity of the membranes in the presence of nanoparticles was much

lower as compared to controls, while at higher temperatures, nanoparticles induced a sharp increase of membrane fluidity.

Membrane fluidity was lowered by the presence of antibiotics alone, for all tested classes of antibiotics. A similar effect was previously reported on artificial membranes [34].

Assuming that the nanoparticles internalization occurs *via* membrane endocytosis, the increased membrane fluidity would favor the rate of antibiotics carriers penetration [35], allowing thus a more efficient drug uptake. According to our results, the membrane fluidity at physiological temperature (37^0C) is influenced specifically in different formulae of drug–nanoparticles systems. There are some cases in which antibiotic–nanoparticle complex increases the membrane fluidity more that the antibiotic alone (amikacin, kanamycin, penicillin, polymyxin, erythromycin, neomycin, streptomycin) making it more favorable for drug penetration. This opens a less toxic alternative for antibiotics administration, shortening the duration of the treatment. The fact that antibiotic functionalized magnetite nanoparticles have a similar biodistribution and tend to localize mainly within the lungs suggest the fact that they may represent an efficient treatment alternative for patients affected by recurrent lung infections [36, 37], which need long-term antibiotics treatments.

Conclusions

Our study reveals that membrane fluidity suffers different changes when a treatment with different class of antibiotics, either used as plain solutions or fused with magnetite nanoparticles is applied. In the case of many used antibiotics, namely amikacin, kanamycin, penicillin, polymyxin, erythromycin, neomycin and streptomycin, it was observed an increase of the membrane fluidity when they were fused with nanoparticles, as compared with plain antibiotic solutions. Antibiotic functionalized magnetite nanoparticles proved a similar biodistribution pattern and were transported through the blood flow. These characteristics, along with the fact that antibiotic functionalized nanoparticles increase the cellular uptake of the drug suggest that they may be used for further studies aiming to develop personalized and more efficient targeted delivery and controlled release nanoshuttles for treating localized and systemic infections.

Acknowledgments

The work has been funded by the Sectoral Operational Programme Human Resources Development 2007–2013 of the Ministry of European Funds through the Financial Agreement POSDRU/159/1.5/S/132397 (ExcelDOC).

References

[1] Kritikou E, *Membrane trafficking: endurance of the weakest signal*, Nat Rev Mol Cell Biol, 2008, 9(10):742–743.
[2] Jou TS, Leung SM, Fung LM, Ruiz WG, Nelson WJ, Apodaca G, *Selective alterations in biosynthetic and endocytic protein traffic in Madin–Darby canine kidney epithelial cells expressing mutants of the small GTPase Rac1*, Mol Biol Cell, 2000, 11(1):287–304.
[3] Alberts B, Johnson A, Lewis J, Raff M, Roberts K, Walter P, *Molecular biology of the cell*, 4th edition, Garland Science, Taylor & Francis Group, New York, 2002.
[4] Grumezescu AM, Gestal MC, Holban AM, Grumezescu V, Vasile BS, Mogoantă L, Iordache F, Bleotu C, Mogoşanu GD, *Biocompatible Fe3O4 increases the efficacy of amoxicillin delivery against Gram-positive and Gram-negative bacteria*, Molecules, 2014, 19(4):5013–5027.
[5] Holban AM, Grumezescu AM, Gestal MC, Mogoanta L, Mogosanu GD, *Novel drug delivery magnetite nano-systems used in antimicrobial therapy*, Curr Org Chem, 2013, 18(2): 185–191.
[6] Gao X, Cui Y, Levenson RM, Chung LWK, Nie S, *In vivo cancer targeting and imaging with semiconductor quantum dots*, Nat Biotechnol, 2004, 22(8):969–976.
[7] Thomas M, Klibanov AM, *Conjugation to gold nanoparticles enhances polyethylenimine's transfer of plasmid DNA into mammalian cells*, Proc Natl Acad Sci U S A, 2003, 100(16): 9138–9143.
[8] Cui Y, Wei Q, Park H, Lieber CM, *Nanowire nanosensors for highly sensitive and selective detection of biological and chemical species*, Science, 2001, 293(5533):1289–1292.
[9] Ferrari M, *Cancer nanotechnology: opportunities and challenges*, Nat Rev Cancer, 2005, 5(3):161–171.
[10] De M, Ghosh PS, Rotello VM, *Applications of nanoparticles in biology*, Adv Mat, 2008, 20(22):4225–4241.
[11] Gupta AK, Naregalkar RR, Vaidya VD, Gupta M, *Recent advances on surface engineering of magnetic iron oxide nanoparticles and their biomedical applications*, Nanomedicine (Lond), 2007, 2(1):23–39.
[12] Kawano T, Yamagata M, Takahashi H, Niidome Y, Yamada S, Katayama Y, Niidome T, *Stabilizing of plasmid DNA in vivo by PEG-modified cationic gold nanoparticles and the gene expression assisted with electrical pulses*, J Control Release, 2006, 111(3):382–389.
[13] Singh B, Hussain N, Sakthivel T, Florence AT, *Effect of physiological media on the stability of surface-adsorbed DNA-dendron-gold nanoparticles*, J Pharm Pharmacol, 2003, 55(12): 1635–1640.
[14] Ehrenberg MS, Friedman AE, Finkelstein JN, Oberdörster G, McGrath JL, *The influence of protein adsorption on nanoparticle association with cultured endothelial cells*, Biomaterials, 2009, 30(4):603–610.
[15] Kong G, Braun RD, Dewhirst MW, *Hyperthermia enables tumor-specific nanoparticles delivery: effect of particle size*, Cancer Res, 2000, 60(16):4440–4445.
[16] Kawai N, Ito A, Nakahara Y, Honda H, Kobayashi T, Futakuchi M, Shirai T, Tozawa K, Kohri K, *Complete regression of experimental prostate cancer in nude mice by repeated hyperthermia using magnetite cationic liposomes and a newly developed solenoid containing a ferrite core*, Prostate, 2006, 66(7):718–727.
[17] Drake P, Cho HJ, Shih PS, Kao CH, Lee KF, Kuo CH, Lin XZ, Lin YJ, *Gd-doped iron-oxide nanoparticles for tumour therapy via magnetic field hyperthermia*, J Mater Chem, 2007, 17(46):4914–4918.
[18] Jordan A, Scholz R, Wust P, Fähling H, Krause J, Wlodarczyk W, Sander B, Vogl T, Felix R, *Effects of magnetic fluid hyperthermia (MFH) on C3H mammary carcinoma in vivo*, Int J Hyperthermia, 1997, 13(6):587–605.
[19] Cho EC, Xie J, Wurm PA, Xia Y, *Understanding the role of surface charges in cellular adsorption versus internalization by selectively removing gold nanoparticles on the cell surface with a I2/KI etchant*, Nano Lett, 2009, 9(3):1080–1084.
[20] Shi X, Thomas TP, Myc LA, Kotlyar A, Baker JR Jr, *Synthesis, characterization, and intracellular uptake of carboxyl-terminated poly(amidoamine) dendrimer-stabilized iron oxide nanoparticles*, Phys Chem Chem Phys, 2007, 9(42):5712–5720.
[21] Conner SD, Schmid SL, *Regulated portals of entry into the cell*, Nature, 2003, 422(6927):37–44.
[22] Villanueva A, Cañete M, Roca AG, Calero M, Veintemillas-Verdaguer S, Serna CJ, Morales Mdel P, Miranda R, *The influence of surface functionalization on the enhanced internalization of magnetic nanoparticles in cancer cells*, Nanotechnology, 2009, 20(11):115103.
[23] Wilhelm C, Billotey C, Roger J, Pons JN, Bacri JC, Gazeau F, *Intracellular uptake of anionic superparamagnetic nanoparticles as a function of their surface coating*, Biomaterials, 2003, 24(6):1001–1011.
[24] Cotar AI, Grumezescu AM, Huang KS, Voicu G, Chifiriuc MC, Radulescu R, *Magnetite nanoparticles influence the efficacy*

of antibiotics against biofilm embedded Staphylococcus aureus cells, Biointerface Res Appl Chem, 2013, 3(2):559–565.
[25] Chifiriuc MC, Grumezescu AM, Andronescu E, Ficai A, Cotar AI, Grumezescu V, Bezirtzoglou E, Lazar V, Radulescu R, *Water dispersible magnetite nanoparticles influence the efficacy of antibiotics against planktonic and biofilm embedded Enterococcus faecalis cells*, Anaerobe, 2013, 22:14–19.
[26] Grumezescu AM, Cotar AI, Andronescu E, Ficai A, Ghitulica CD, Grumezescu V, Vasile BS, Chifiriuc MC, *In vitro activity of the new water-dispersible Fe3O4@usnic acid nanostructure against planktonic and sessile bacterial cells*, J Nanopart Res, 2013, 15:1766.
[27] Lakowicz JR, *Principles of fluorescence spectroscopy*, 2nd edition, Kluwer Academic/Plenum Publishers, New York, 1999, 185–210.
[28] Mogoşanu GD, Popescu FC, Busuioc CJ, Lascăr I, Mogoantă L, *Comparative study of microvascular density in experimental third-degree skin burns treated with topical preparations containing herbal extracts*, Rom J Morphol Embryol, 2013, 54(1):107–113.
[29] Voicu G, Anghel AG, Badea M, Bordei E, Crantea G, Gavrilă RI, Grecu A, Jercan DAM, Nicolae BC, Vochiţoaia GC, Tchinda K, Holban AM, Bleotu C, Grumezescu AM, *Silica network improve the effect of fludarabine and paclitaxel on HCT8 cell line*, Rom J Morphol Embryol, 2014, 55(2 Suppl):545–551.
[30] Voicu G, Crică LE, Fufă O, Moraru LI, Popescu RC, Purcel G, Stoilescu MC, Grumezescu AM, Bleotu C, Holban AM, Andronescu E, *Magnetite nanostructures functionalized with cytostatic drugs exhibit great anti-tumoral properties without application of high amplitude alternating magnetic fields*, Rom J Morphol Embryol, 2014, 55(2):357–362.
[31] Holban AM, Grumezescu V, Grumezescu AM, Vasile BŞ, Truşcă R, Cristescu R, Socol G, Iordache F, *Anti-microbial nanospheres thin coatings prepared by advanced pulsed laser technique*, Beilstein J Nanotechnol, 2014, 5:872–880.
[32] Anghel AG, Grumezescu AM, Chirea M, Grumezescu V, Socol G, Iordache F, Oprea AE, Anghel I, Holban AM, *MAPLE fabricated Fe3O4@Cinnamomum verum antimicrobial surfaces for improved gastrostomy tubes*, Molecules, 2014, 19(7):8981–8994.
[33] Brown RC, Silver AC, Woodhead JS, *Binding and degradation of NH2-terminal parathyroid hormone by opossum kidney cells*, Am J Physiol, 1991, 260(4 Pt 1):E544–E552.
[34] Kovács E, Savopol T, Iordache MM, Săplăcan L, Sobaru I, Istrate C, Mingeot-Leclercq MP, Moisescu MG, *Interaction of gentamicin polycation with model and cell membranes*, Bioelectrochemistry, 2012, 87:230–235.
[35] Rhode S, Grurl R, Brameshuber M, Hermetter A, Schütz GJ, *Plasma membrane fluidity affects transient immobilization of oxidized phospholipids in endocytotic sites for subsequent uptake*, J Biol Chem, 2009, 284(4):2258–2265.
[36] Gibson RL, Burns JL, Ramsey BW, *Pathophysiology and management of pulmonary infections in cystic fibrosis*, Am J Respir Crit Care Med, 2003, 168(8):918–951.
[37] Saiman L, Siegel J, *Infection control in cystic fibrosis*, Clin Microbiol Rev, 2004, 17(1):57–71.

Corresponding author
Alexandru Mihai Grumezescu, Chem. Eng., PhD, Department of Science and Engineering of Oxide Materials and Nanomaterials, Faculty of Applied Chemistry and Materials Science, Politehnica University of Bucharest, 1–7 Polizu Street, 011061 Bucharest, Romania; Phone +4021–402 39 97, e-mail: grumezescu@yahoo.com

Received: May 18, 2014

Accepted: September 19, 2014